

Phase Separation of Saturated and Mono-unsaturated Lipids as determined from a Microscopic Model

R. Elliott, K. Katsov, and M. Schick

*Department of Physics, University of Washington,
Box 351560, Seattle, WA 98195-1560 U. S. A.*

I. Szleifer

*Department of Chemistry, Purdue University,
West Lafayette, IN 47907-1393 U. S. A.*

(Dated: October 15, 2018, draft)

Abstract

A molecular model is proposed of a bilayer consisting of fully saturated DPPC and mono unsaturated DOPC. The model not only encompasses the constant density within the hydrophobic core of the bilayer, but also the tendency of chain segments to align. It is solved within self-consistent field theory. A model bilayer of DPPC undergoes a main chain transition to a gel phase, while a bilayer of DOPC does not do so above zero degrees centigrade because of the double bond which disrupts order. We examine structural and thermodynamic properties of these membranes and find our results in reasonable accord with experiment. In particular, order-parameter profiles are in good agreement with NMR experiments. A phase diagram is obtained for mixtures of these lipids in a membrane at zero tension. The system undergoes phase separation below the main-chain transition temperature of the saturated lipid. Extensions to the ternary DPPC, DOPC, and cholesterol system are outlined.

I. INTRODUCTION

The hypothesis that the lipids in the plasma membrane are distributed inhomogeneously has received enormous attention. Small domains, known as “rafts”, rich in saturated lipids and cholesterol, have been implicated in many biological processes including endocytosis, transcription and transduction processes, and viral infection. The size and nature of such domains in biological membranes is currently unclear¹. The situation in model membranes, however, is more transparent. Experimental studies in giant unilamellar vesicles^{2,3,4} containing mixtures of saturated and unsaturated lipids and cholesterol, which mimic the components of the outer leaflet of the plasma membrane, show the existence of at least three phases; a saturated lipid-rich gel phase, a saturated lipid and cholesterol-rich liquid phase, and an unsaturated lipid-rich liquid phase. The two liquid phases coexist in some regions of the phase diagram. The sensitivity of the phase separation to the components and their composition is demonstrated by the fact that mixtures of unsaturated lipids and cholesterol, mimicking the components of the inner leaflet of the plasma membrane, do not phase separate⁵.

Theoretical consideration of mixtures of lipids and cholesterol have been carried out on binary mixtures of saturated lipids and cholesterol using models in which the enormous numbers of degrees of freedom of the lipids are severely reduced. In spite of this simplification, these models have demonstrated the importance of the preferential interaction between cholesterol and saturated lipids in bringing about a “liquid ordered” phase in which the tails are relatively well-ordered^{6,7}.

It is our contention that two conditions are sufficient for bringing about coexistence between a cholesterol and saturated lipid-rich liquid ordered phase and an unsaturated lipid-rich “disordered liquid” in which the tails are typically disordered. The first of these is that the system be below the main-chain transition of the saturated lipid to its gel phase, a transition driven by the ordering of the lipid tails. This transition is first-order, and is characterized by discontinuities in those thermodynamic quantities which are first derivatives of the free energy with respect to its arguments; *e.g.* the entropy, the area per head group, etc. In particular, upon introduction of an unsaturated lipid, discontinuities arise in the areal densities of the two lipids, first derivatives of the free energy with respect to the chemical potentials. In other words, phase separation between a saturated lipid-rich gel phase and

an unsaturated lipid-rich disordered liquid phase is a simple consequence of the main-chain transition. The difference in component concentrations in the two phases is expected to be large because the presence of the *cis* double bond causes the unsaturated chains to pack poorly with the saturated chains that are well-ordered in the gel phase. It also follows from the first-order nature of the main chain transition that the addition of cholesterol to the saturated lipid will result in a phase separation between a saturated lipid-rich gel phase and a liquid phase of lipid and cholesterol. Whether this liquid phase will coexist with the disordered liquid phase or simply transform smoothly to it as the composition of a ternary mixture changes depends on how different the liquids are. Thus the second sufficient condition for liquid-liquid phase separation is, as noted above, that the cholesterol favor increased ordering of the saturated lipid tails, so that the disordered tails of the unsaturated lipid will also tend to be expelled from the ordered fluid causing coexistence between it and an unsaturated-rich disordered fluid.

In this paper, we consider a mixture of saturated and unsaturated lipids within a bilayer and show, as contended above, that below the main chain transition of the saturated lipid, there is a demixing phase separation. We do this in a model in which the lipid tails are treated microscopically according to the rotational isomeric states model of Flory⁸ which permits each CH_2 group to be in one of three configurations; the lowest energy *trans*, or thermally excited *gauche plus* or *gauche minus*. In the latter, the chain configuration exhibits a kink. Due to thermal excitation and de-excitation, this kink is transient in contrast to that in the unsaturated chain which is permanent. To model much of the effect of the interactions between the lipid segments, we follow early work^{9,10} and constrain the density of the bilayer interior to be constant, equal to a value typical of its oily components. As shown by these authors, imposition of this packing constraint causes the system to exhibit a single disordered liquid phase, characterized by a certain average number of *gauche* bonds per chain, and a certain area per chain. Larger areas could be attained by increasing the average number of *gauche* bonds in the chains, but this increases the energy and free energy of the system. Smaller areas could be attained by eliminating even more *gauche* bonds, but this decreases the chain entropy to the point that the free energy again increases. Thus the observed liquid phase occurs at an areal density at which an incremental decrease in entropy of the chains is just compensated by an incremental reduction in energy of *gauche* bonds¹¹.

The constant density constraint is not adequate to bring about the main-chain transition

to a gel phase, a transition which, we have argued, is one of the sufficient conditions for raft formation. In order to bring about *both* liquid and gel phases, we not only impose the constant density constraint, but also include a local orientational interaction between normals to the CH_2 planes of adjacent chains, one which tends to align them. We expect that inclusion of this explicit orientational interaction will capture the aligning tendency of the inter-chain packing. Indeed we find that this interaction does bring about a second minimum in the free energy, one characterized by fewer gauche bonds than in the liquid phase, and which we identify therefore, with the gel phase. In contrast to the liquid phase, an incremental reduction in entropy of the more ordered chain conformations is compensated here by an incremental decrease in orientational energy.

We first consider a single component system of saturated tails consisting of fifteen monomeric segments, modeling those of dipalmitoylphosphatidylcholine, (DPPC). We find a first-order main chain transition at a temperature, T_m , and calculate the degree of segment order as a function of position down the chain, and find good agreement with experiment. There is a concomitant change in area per head group as the chains lengthen in the gel phase. Next, we apply our technique to a bilayer of unsaturated lipids. The unsaturated chains we consider are seventeen monomeric units long, with a *cis*- double bond located between monomers eight and nine. This resembles the chain structure of dioleoylphosphatidylcholine, (DOPC). We find no transition for bilayers composed only of this unsaturated lipid above the melting point of water. Finally, we consider a mixture of these saturated and unsaturated chains. At temperatures below T_m , the system phase separates into a saturated lipid-rich gel phase and an unsaturated lipid-rich disordered liquid phase. Although there is little experimental data on this mixture, we find acceptable agreement with that which exists.

This paper is organized as follows. In the next section, we introduce the theory for a bilayer slab composed of a mixture of two lipid tails, one saturated and one unsaturated, and also introduce the interaction we employ for this system. With these definitions, the partition function for the full mixture is specified. It is then calculated within the framework of self-consistent field theory in Appendix I. Central to this theory are two self-consistent equations which specify two local, effective fields. The first enforces the constant-density constraint, and the second tends to align the local chain segment orientation. This subsection is written for a general system of two lipid species, one with identical saturated tails, the other

with identical unsaturated tails. In the following subsection, we introduce the microscopic model we use to describe the lipid tails.

In section III, the general theory is applied to two specific lipids, DOPC and DPPC. We first consider two different pure bilayers, those composed of only one or the other of these lipids. We present results pertinent to the main-chain transition in the DPPC bilayer and some geometric, conformational, and thermodynamic statistics of these membranes calculated in the context of our model. Of note are the deuterium order parameters for these lipids since they indicate the acyl chain's average conformation in the bilayer due to packing with neighboring lipids. In the final subsection, we present the phase diagram for the system of mixed lipid bilayers and some conformational statistics calculated in this model.

II. THE MODEL AND ITS SELF-CONSISTENT FIELD SOLUTION

A. Theory

We consider a bilayer membrane of area A composed of N_s saturated and N_u unsaturated lipids whose tails occupy a volume V , the total volume of the hydrophobic core of both bilayer leaflets. Head groups are placed symmetrically, facing the external, aqueous environment of solvent. Temporarily, we ignore all interactions between head groups and the solvent molecules focusing only on the hydrophobic core of the bilayer. Acyl tails are tethered to the glycerol backbone of the lipid head groups on both sides of the bilayer, and the first monomer segments extending from the backbone define the interfaces of the hydrophobic core. The full width of this hydrophobic core, including both leaflets, is L . The system of acyl tails comprising the hydrophobic core is treated as incompressible. This assumption constrains the average density of monomers to a constant liquid-like value throughout the bilayer. The total volume is simply the sum of all monomer volumes.

In the following, we limit our attention to lipids consisting of two identical tails. We further simplify the system to that of a mixture of the individual, interacting chains rather than a system of chain pairs extending from a common headgroup. This should make little difference to the chain conformations because the chains are so tightly packed¹².

The saturated lipid has the tail structure, $P-(CH_2)_{n_s-1}-CH_3$, which we model as a chain of n_s linked segments extending from the glycerol backbone labeled P . All monomers except

the last are CH_2 segments with monomeric volumes $\nu_s(k) = \nu_0 = 28\text{\AA}^3$, $k = 1, n_s - 1$. The last monomer is a CH_3 segment, which is assigned a volume $\nu_s(n_s) = 2\nu_0^{13,14,15}$. Other than these volumes, the monomers are without structure, and spaced a bond length of $l_0 = 1.53\text{\AA}$ apart. The microscopic monomer number density of the saturated lipid, averaged over the plane of the bilayer, is

$$\hat{\Phi}_s(z, \Sigma) = \frac{1}{A} \sum_{\gamma}^{N_s} \hat{\phi}_{s,\gamma}(z, \alpha_{\gamma}), \quad (1)$$

$$\hat{\phi}_{s,\gamma}(z, \alpha_{\gamma}) = \sum_{k=1}^{n_s} \nu_s(k) \delta(z - z_{k,\gamma}(\alpha_{\gamma})), \quad (2)$$

where $z_{k,\gamma}(\alpha_{\gamma})$ is the z coordinate of the k 'th monomer of the γ 'th saturated chain when the chain is in the configuration α_{γ} . The circumflex denotes that a quantity depends upon the lipid configuration. Here the single chain density, $\hat{\phi}_{s,\gamma}$, depends upon the single chain configuration α_{γ} , and the total chain density, Φ_s depends upon the configuration Σ of all the lipids. For typographical convenience, we will simply write $\hat{\Phi}_s(z)$ henceforth, suppressing the explicit dependence on the lipid configurations and allowing the circumflex to remind the reader of this dependence. We average over the plane of the bilayer as we shall be considering phases which are translationally invariant in this plane.

The unsaturated lipid tail is similarly constructed of n_u linked monomers. It has the tail structure $P - (CH_2)_x - CH = CH - (CH_2)_y - CH_3$, which is a monounsaturated chain of $n_u = x + 2 + y + 1$ segments. Each CH_2 and CH_3 segment is assigned a volume identical to that in the saturated lipid; each half of the $-CH = CH-$ segment of the *cis*-unsaturated bond is assigned a volume of $\nu_{CH} = 0.8\nu_0^{14}$. The microscopic monomer number density of the unsaturated lipid tails is, then,

$$\hat{\Phi}_u(z) = \frac{1}{A} \sum_{\zeta}^{N_u} \hat{\phi}_{u,\zeta}(z) \quad (3)$$

$$\hat{\phi}_{u,\zeta}(z) = \sum_{j=1}^{n_u} \nu_u(j) \delta(z - z_{j,\zeta}), \quad (4)$$

with volume weights,

$$\nu_u(j) = \begin{cases} \nu_0 & \text{if } j \leq x \text{ or } x + 2 < j < n_u \\ 0.8\nu_0 & \text{if } j = x + 1, x + 2 \\ 2\nu_0 & \text{if } j = n_u. \end{cases} \quad (5)$$

With these monomer volumes, the total hydrophobic volumes of single DMPC, DPPC, and DOPC lipids are 784\AA^3 , 896\AA^3 and 985.6\AA^3 , respectively, which agree well with the experimental values of 782\AA^3 , 913\AA^3 and 984\AA^3 for the fluid phases¹⁵. We assume these monomeric volumes have no dependence on temperature.

Much of the effect of the long-range van der Waals attraction and hard core repulsion is taken into account by the incompressibility constraint. This is clear from the agreement between results obtained with this approximation and molecular dynamics simulation for the liquid phases^{9,12}. However an approximation based on density alone cannot capture the enhanced alignment of the tails which drives the main chain transition. For this we will need to know the local alignment of the chains. Our presumption is that the microscopic interactions within the system favor those configurations in which the tails are more aligned with one another because in such configurations the chains are more efficiently packed. We shall include a pairwise interaction \mathcal{E} between chains that reflects this assumption.

The local orientation of the chains is conveniently specified by the normal to the local CH_2 group. In particular, the normal to the plane determined by the k 'th CH_2 group on chain γ can be written

$$\mathbf{u}_{k,\gamma} = \frac{\mathbf{r}_{k-1,\gamma} - \mathbf{r}_{k+1,\gamma}}{|\mathbf{r}_{k-1,\gamma} - \mathbf{r}_{k+1,\gamma}|}, \quad k = 1 \dots n_s - 1. \quad (6)$$

The position vector of the anchoring carbon of chain γ is denoted $\mathbf{r}_{0,\gamma}$. Subsequently we shall refer to the $\mathbf{u}_{k,\gamma}$ simply as “normals”, or “orientation vectors”.

It is now convenient to introduce a local density of these normals¹⁶ which, for the saturated lipid is,

$$\hat{\Psi}_s(z, \mathbf{u}) = \frac{1}{A} \sum_{\gamma} \sum_{k=1}^{n_s-1} \nu_s(k) \delta(z - z_{k,\gamma}) \delta(\mathbf{u} - \mathbf{u}_{k,\gamma}). \quad (7)$$

Again the circumflex is a reminder that this density depends explicitly on the chain coordinates $z_{k,\gamma}$ and normals $\mathbf{u}_{k,\gamma}$ in a particular configuration of lipids. There is a similar expression, $\hat{\Psi}_u$ for the local density of normals coming from unsaturated chains.

A local pairwise interaction between tail segments which depends upon their orientations can be written,

$$\mathcal{E}[\hat{\Psi}_s, \hat{\Psi}_u] = \frac{A}{2\nu_0} \int dz \int d\mathbf{u} d\mathbf{u}' [\hat{\Psi}_s(z, \mathbf{u}) + \hat{\Psi}_u(z, \mathbf{u})] V(\mathbf{u}, \mathbf{u}') [\hat{\Psi}_s(z, \mathbf{u}') + \hat{\Psi}_u(z, \mathbf{u}')]. \quad (8)$$

Here, $\int d\mathbf{u}$ denotes an integration over the full solid angle. It is important to note that all interactions are local, *i.e.* between bonds, and are of the same form and strength irrespective of the length or degree of unsaturation of the chains to which the bonds belong.

Because the normal to the plane of the bilayer, \mathbf{c} , singles out a spatial direction, we expect the interaction to depend upon the angles that the segments make with this normal $V(\mathbf{u}, \mathbf{u}') = V(\mathbf{u}', \mathbf{u}) \rightarrow V(\mathbf{u} \cdot \mathbf{c}, \mathbf{u}' \cdot \mathbf{c})$. Irrespective of the particular form chosen for this interaction, within the mean-field approximation which we introduce shortly, the dependence of the free energy of a single chain on the normal can only arise through functions of $\mathbf{u} \cdot \mathbf{c}$. It follows from this and the fact that the interaction energy, \mathcal{E} , is pairwise that the free energy of the system of chains can only depend upon a product of such functions. Anticipating this, we take for the interaction a simple form which already exhibits this product nature,

$$V(\mathbf{u} \cdot \mathbf{c}, \mathbf{u}' \cdot \mathbf{c}) \approx -Jf(\mathbf{u} \cdot \mathbf{c})f(\mathbf{u}' \cdot \mathbf{c}) = -Jf(\cos \theta)f(\cos \theta'), \quad (9)$$

where $f(\cos \theta)$ is normalized. Further, in the absence of headgroup interactions which we have ignored, the chains will align normal to the plane of the bilayer which implies that $f(\cos \theta)$ be chosen a monotonically decreasing function of its argument. With this orientational interaction, the lowest energy configuration of two neighboring orientational vectors is one in which they avoid the penalty of hard-core interaction by both aligning with the bilayer normal.

With this choice of orientational interaction, it is convenient to define

$$\begin{aligned} \hat{\Xi}_s(z) &\equiv \int d\theta \sin \theta \hat{\Psi}_s(z, \mathbf{u}) f(\mathbf{u} \cdot \mathbf{c}) \\ &= \frac{1}{A} \sum_{\gamma=1}^{N_s} \hat{\xi}_{s,\gamma}(z), \end{aligned} \quad (10)$$

$$\hat{\xi}_{s,\gamma}(z) = \sum_{k=1}^{n_s-1} \nu_s(k) \delta(z - z_{k,\gamma}) f(\mathbf{u}_{k,\gamma} \cdot \mathbf{c}), \quad (11)$$

with a similar expression for the unsaturated lipid tails, so that the interaction energy can be written in the transparent form,

$$\mathcal{E} = -\frac{JA}{2\nu_0} \int dz [\hat{\Xi}_s(z) + \hat{\Xi}_u(z)]^2. \quad (12)$$

For $f(\cos \theta)$ we choose the simple functional form

$$\begin{aligned} f(\cos \theta) &= \frac{2m+1}{2} (\cos^2 \theta)^m \\ &\approx m \exp(-m\theta^2), \end{aligned} \quad (13)$$

which is approximately a Gaussian with width $m^{-\frac{1}{2}}$. The prefactor is a normalization coefficient. If the interaction, Eq. (12), were not local but were an average over the lipid chain, and if m were unity in the expression above, then this interaction would be comparable to the leading order term of the interaction Marcelja¹⁷ considered for saturated lipids. The local form, and higher power dependence of the alignment with the bilayer normal was first considered by Gruen¹⁰.

Two parameters determine this interaction between segments, its strength J and its angular range. The former is set by requiring that the main-chain transition temperature for the chains under consideration agree with experiment. The latter may be estimated by considering the average angular alignment of an acyl tail in the bilayer. Crudely, a lipid in the bilayer is, on average, confined to a cylindrical shape. A simple estimate of its alignment with the normal is then $\theta_0 \sim \bar{a}^{\frac{1}{2}}/\bar{l}$, where \bar{a} is an average cross-sectional area for an acyl chain and \bar{l} is an average length in a typical membrane leaf. Comparison of the Gaussian width to this estimate, leads to $m \sim 14 - 18$. We use $m = 18$ in our calculations.

Now that the interactions between chains are defined, the Helmholtz free energy of the system, subject to the incompressibility constraint of constant density, can be obtained within self-consistent, or mean field, theory. This is done in Appendix I with the result

$$\begin{aligned} \frac{\beta F_{mft}(T, N_s, N_u, A)}{A} &= -\rho_s \ln Q_s - \rho_u \ln Q_u + \frac{\beta J}{2\nu_0} \int dz [\rho_s \langle \hat{\xi}_s(z) \rangle_s + \rho_u \langle \hat{\xi}_u(z) \rangle_u]^2 \\ &+ \frac{\rho_s}{2} \ln \frac{\rho_s \nu_0}{\rho_s \sum_k \nu_s(k) + \rho_u \sum_k \nu_u(k)} + \frac{\rho_u}{2} \ln \frac{\rho_u \nu_0}{\rho_s \sum_k \nu_s(k) + \rho_u \sum_k \nu_u(k)} \\ &- \frac{1}{\nu_0} \int dz \pi(z), \end{aligned} \quad (14)$$

where $\rho_s \equiv N_s/A$ and $\rho_u \equiv N_u/A$ are the areal densities of saturated and unsaturated chains. Here $\langle \hat{\xi}_s(z) \rangle_s$ is the average in the ensemble of a single saturated chain

$$\langle \hat{\xi}_s(z) \rangle_s \equiv Tr_{\{\alpha\}} P_s \hat{\xi}_s(z) \quad (15)$$

where the trace is over all configurations of a single saturated chain, and the probability distribution P_s is given by

$$P_s = \frac{1}{Q_s} \exp \left\{ -\beta \hat{H}_1 - \frac{1}{\nu_0} \int [\hat{\phi}_s(z) \pi(z) + \hat{\xi}_s(z) b(z)] dz \right\} \quad (16)$$

with Q_s the single saturated chain partition function

$$Q_s(\pi, b) = Tr_{\{\alpha\}} \exp \left\{ -\beta \hat{H}_1 - \frac{1}{\nu_0} \int [\hat{\phi}_s(z) \pi(z) + \hat{\xi}_s(z) b(z)] dz \right\}, \quad (17)$$

and \hat{H}_1 the intra-chain part of the Hamiltonian. The self-consistent equations which determine the fields $\pi(z)$ and $b(z)$ are

$$1 = \rho_s \langle \hat{\phi}_s(z) \rangle_s + \rho_u \langle \hat{\phi}_u(z) \rangle_u, \quad (18)$$

$$b(z) = -\beta J [\rho_s \langle \hat{\xi}_s(z) \rangle_s + \rho_u \langle \hat{\xi}_u(z) \rangle_u]. \quad (19)$$

The first of these enforces the incompressibility constraint.

Note that, because of the incompressibility constraint, the volume is not an independent variable so that the Helmholtz free energy, Eq. (14), depends only on the temperature, the numbers of each lipid, and the area. The interpretation of the free energy is straightforward. The first two terms are simply the single chain Gibbs free energies multiplied by the number of chains per unit area. As is well known, these terms double-count the pairwise interaction energy, and this is corrected by the third term. The next two terms are the entropy of mixing, and the last is simply $-\beta pV/A$ which relates the Gibbs free energy of the preceding terms to a Helmholtz free energy.

Other than excluding tail configurations protruding into the solvent region, the effects of the aqueous medium and head groups have thus far been neglected. It is evident that the interfacial effects can also be somewhat complex. For example, tilted solid phases are often attributed to a mismatch between a smaller average areal footprint of the packed tails and a larger headgroup. On the other hand, a small headgroup mismatched with larger, fluid-like tails attached to it can yield costly interfacial interactions between the solvent and the hydrophobic core, resulting in a large interfacial tension. These effects are beyond the scope of our calculation. However, so as not to overlook the contributions from the head groups completely, we choose a minimal model for them.

Ignoring the molecular details of the head groups and their interactions with the aqueous environment, we focus on two physical attributes that result from these interactions. The first is an interfacial energy per unit area, which we include as a simple phenomenological form, $\gamma_0 A$. Thus the total free energy per unit area is

$$f_A(T, \rho_s, \rho_u) = F_{mft}/A + \gamma_0, \quad (20)$$

where F_{mft} is given in Eq. (14). The value of γ_0 is taken to be on the order of the energy per unit area of an oil-water interface. We use $\gamma_0 = 0.12k_B T/\text{\AA}^2$ in our calculations, which is roughly the experimental value. The second effect attributable to the head groups is the

rigidity they provide the acyl tail. The lipid tails are tethered to the glycerol backbone, providing a fixed endpoint for the chain. The head groups tend to order the first segments of the lipid tethered there, an effect which we model by a surface field that couples to the first bond of the lipid. To model this, we include in \hat{H}_1 a surface field term $\eta \cos(\mathbf{u}_1 \cdot \mathbf{c})$. The magnitude of the surface field η is tuned so that the average angle of the first bond is approximately equal to that obtained from NMR measurements for the lipid.

B. Microscopic Model

To evaluate the single lipid partition function in external fields, Eq. (17) above, we specify a microscopic model suitable for describing the noninteracting single chain configurations and their energy, \hat{H}_1 . To this end, we employ Flory’s Rotational Isomeric States (RIS) model⁸ for the lipid acyl chains. This model places a subsequent monomer in the acyl chain at one of three discrete possible orientations from its ancestor segment; the trans, gauche plus, and gauche minus orientations. According to this model, the gauche bonds are local excitations that contort the chain and increase the energy by $\epsilon_g = 500$ cal/mol. Thus \hat{H}_1 of a given configuration is simply equal to ϵ_g multiplied by the number of gauche bonds in that configuration, and also includes the contribution from the surface field described above. The lipid conformation with all trans bonds is a highly stretched chain, whereas a lipid tail with several gauche bonds is coiled. Given the location of the first bond in the acyl chain, all positions of the subsequent $n_s - 1$ generations are determined by this model, which locates segments in a tetrahedral fashion, with skeletal angles of 112° , and dihedral angles of $\{0^\circ, \pm 120^\circ\}$ for trans and gauche \pm orientations respectively. Without restrictions on this set, there are 3^{n_s-1} configurations for each fixed, first bond orientation.

The *cis*- double bond in the unsaturated chains slightly modifies this model. This bond is a quenched defect in the chain, effectively placing a kink in the tail about the location of the double bond. The energies and configurations of the segments adjoining the double bond as well as the $-C = C-$ bond length differ slightly from the saturated links. For the segments associated with the double bond, we employ the RIS configurational model of *cis*-1,4-polybutadiene¹⁸, which possesses the same atomic structure as the double bonds in these lipid chains.

We also impose several restrictions on the lipid configurations that reduce the number

of allowed ones significantly. First of all, configurations that protrude into the aqueous environment are discarded. A configuration with any two, non-consecutive monomer centers less than a bond width apart is considered self-intersecting and also discarded. Configurations with consecutive gauche minus (plus), gauche plus (minus) bond sequences have large hydrogen-hydrogen steric overlaps⁸, a phenomena referred to as the “pentane effect.” These configurations are also neglected. Each single lipid partition function is then evaluated by enumerating all allowed configurations in the RIS model, from many different first bond orientations and locations. It should be noted that two different first segment orientations will have different numbers of configurations stemming from them since they will have different number of configurations that penetrate the aqueous environment.

We specify in Appendix II how the probability distributions P_s and P_u and the single lipid partition functions, Eq. (17), are calculated within the context of the RIS model and the configurational restrictions. We also discuss there a few other details of the calculation of the free energy.

III. RESULTS

A. Single component DPPC and DOPC bilayers

We first apply our method to a tensionless bilayer composed only of DPPC lipids. We solve the self-consistent equations for a given temperature and under the condition that the surface tension be zero. The high temperature liquid phase undergoes a main chain transition to a low temperature gel phase, and by adjusting the interaction strength J , we set this transition temperature at $T_m \sim 315$ K, essentially the experimental one¹⁹. The value of J remains fixed at this value throughout all subsequent calculations. In Fig. 1 we show the Helmholtz free energy *per two-chain lipid*

$$f_{N_s}(T, a_s) = 2 \left(\frac{F_{mft}}{N_s} + \gamma_0 a_s \right) \quad (21)$$

in units of $k_B T$ plotted *vs.* the area per two-chain lipid, $2A/N_s = 2a_s$, at the temperature of the main chain transition. It is straight forward to show that

$$f_{N_s}(T, a_s) = 2(\mu_s + \gamma a_s) \quad (22)$$

$$df_{N_s} = 2[\gamma da_s - (S/N_s)dT], \quad (23)$$

with S the total entropy. The two minima in the figure occur at the areal densities of the two coexisting phases. Because these states are minima of the free energy per lipid, their surface tensions vanish, as seen from Eq. (23). Further as they have the same free energy per lipid at zero surface tension, they have the same chemical potential, as seen from Eq. (22). Thus these phases are indeed at coexistence. The main chain transition is clearly seen to be first order, marked by a discontinuous jump in the area per lipid. Table I summarizes a few geometric aspects of each state and of the transition. We find satisfactory agreement with experiment for the geometric properties. The fluid phase is characterized by a greater area per lipid than is the gel phase. The hydrophobic width of the bilayer is thinner, filled with coiled lipid tails with, on average, somewhat more than four gauche bonds per tail. The gel state consists of more ordered lipid chains that are tightly packed, having a smaller area per lipid and fewer gauche bonds.

One thermodynamic quantity that is sensitive to the packing in the hydrophobic core is the deuterium “ S_{CD} ” order parameter profile, which is commonly measured in the fluid state by nuclear magnetic resonance (NMR) experiments. The calculated deuterium order parameter for our model DPPC bilayer is shown in Fig. 2 for both fluid and gel states. The fluid phase is compared to experimental data from reference 20. Collective organization of the lipid tails during the transition from the fluid to gel state is indicated by the large jump in chain alignment. Experiment and simulation distinguish $sn - 1$ and $sn - 2$ lipid tails, which we do not, so the calculated profiles in Fig. 2 should be considered as an average over both acyl tails. Comparing to experiment, we see that the calculated fluid phase is slightly more disordered than the experimental one.

Applying our calculational method to a bilayer consisting only of mono-unsaturated, DOPC model lipids, we find a fluid phase and no transition above the freezing point of water. This result is consistent with experiment, which indicates a transition temperature for DOPC of $T_m \sim 250$ K. The calculated fluid state has an area per lipid of 70.4\AA^2 and a hydrophobic width of 28.0\AA . This lipid area is somewhat smaller than the experimental value of 72.5\AA^2 with also a thinner hydrophobic width of 27.1\AA . The calculated deuterium order parameter is shown in Fig. 2. It should be noted that these profiles are calculated for a lower temperature, $T = 305$ K, than the saturated lipids. The order parameter displays a notch in the profile about the *cis*- double bond, one which is also seen in MD simulation^{20,21,22}. Also, there is a slight even-odd effect in the order parameter which we do not observe in the

saturated chains.

B. Composite bilayers of DPPC and DOPC

From the calculation of the free energy, Eq. (14), the phase behavior for a mixture of both lipids, DPPC and DOPC, can be determined. Phase coexistence is determined by examining the auxiliary function,

$$\tilde{\gamma} = \min_{\rho_s, \rho_u} \{f_A - \lambda_s \rho_s - \lambda_u \rho_u\}. \quad (24)$$

When the λ_s and λ_u are adjusted so that $\tilde{\gamma}$ exhibits two minima with the same value of $\tilde{\gamma}$, then there is two-phase coexistence. At this point, the values of λ_s , λ_u are equal to the values of the chemical potentials of the saturated and of the unsaturated lipids, μ_s and μ_u , in the coexisting phases and $\tilde{\gamma}$ is equal to the surface tension, γ , of each phase. We further require that this surface tension be zero in each phase as there is no constraint on the bilayer area. The four requirements that the chemical potentials and surface tension be equal in each phase and that the tension be zero determines the two areal densities, ρ_s and ρ_u , in each of the two phases. Note that the bare surface tension, γ_0 , causes the system to contract to the point at which the tension due to packing just counteracts the bare tension leaving a net tension of zero.

The calculated phase diagram of the system is shown in Fig. 3. For small concentrations of DOPC, we find a gel state rich in DPPC below the main-chain transition temperature. A region of fluid/gel coexistence is found which is rather wide because of the poor packing of the unsaturated lipids. These results are in reasonable agreement with experiment²³.

The deuterium order parameters for the two coexisting phases at $T = 293$ K are shown in Fig. 4. The gel phase shows significant ordering of both lipids, given by the large absolute magnitude of both order parameters. The disordering effect of the double bond is more prominent in the ordered phase, with affected bonds showing a large notch. This is noteworthy because it implies that the tight packing about the unsaturated lipids in the ordered phase tends to *enhance* the disorder about the unsaturated bond. The order parameters in the liquid-crystalline phases are also shown in Fig. 4.

IV. SUMMARY

We have formulated a microscopic model of a bilayer consisting of lipids, one which incorporates two important effects of the interactions between chains; the tendency of the chains to create an incompressible hydrophobic interior, and their cooperative tendency to order. The solution of the model obtained from self-consistent field theory reproduces many salient features of the lipid bilayer. The system of chains which mimic DPPC undergoes a first-order main chain transition from a disordered fluid state to a more ordered gel phase, a transition characterized by a reduction in the number of gauche bonds and the area per chain. The ordering of the chains in the liquid phase as determined by the deuterium order parameter is in rather good agreement with experiment. We have also calculated the deuterium order parameter in the gel phase.

We then applied the model to a system mimicking the mono-unsaturated chains of DOPC. Utilizing the same interaction as before, we find that this system does not undergo a main chain transition above zero degrees centigrade, a result in agreement with experiment. The lowering of the main-chain transition is due to the double bond in the chain which disrupts the tendency to order. The deuterium order parameter profiles for this system show the characteristic reduction at the position of the double bond.

Lastly we examined a mixture of saturated and unsaturated lipids and showed that the system phase separates into a saturated-lipid-rich gel phase and an unsaturated-lipid-rich liquid phase at temperatures below the main-chain transition temperature of the saturated lipid. The separation arises from the first-order main chain transition. The large difference in areal densities is due to the lipid architecture; the unsaturated lipids are rejected from the gel phase because they do not pack into it very well.

Several pieces of physics have been ignored in our calculation, such as the explicit interaction between head groups and, of course, the effect of fluctuations. We expect that such effects will alter the specific values of thermodynamic quantities, but not the main phenomena. In particular the phase separation into a saturated-rich gel and an unsaturated -rich liquid phase will remain below the main chain transition of the saturated lipid. As noted earlier, this is important as this behavior is one of two ingredients for a sufficient theory of liquid-liquid coexistence in a ternary mixture which includes cholesterol. We are currently investigating the role of this third component within the framework of our model.

V. ACKNOWLEDGMENTS

We thank Sarah Veatch, Sarah Keller, Ben Stottrup, Kazuya Okubo, and Marcus Müller for stimulating conversations, and Avinoam Ben-Shaul for helpful correspondence.

This material is based upon work supported by the National Science Foundation under Grants No. 140500 and CTS-0338377, and in part by a National Science Foundation IGERT fellowship from the University of Washington Center of Nanotechnology.

VI. APPENDIX I. SELF-CONSISTENT FIELD THEORY

The exact Helmholtz free energy of the system is

$$F = Tr_{\{\Sigma\}} P_{ex} \left[H + \beta^{-1} \ln P_{ex} \right] \quad (25)$$

where the trace is a sum over all distinguishable configurations of all chains, two chains per molecule, and P_{ex} is the exact probability distribution function for the system. It satisfies

$$Tr_{\{\Sigma\}} P_{ex} = 1. \quad (26)$$

The Hamiltonian of the system is

$$H = \sum_{\gamma=1}^{N_s} \hat{H}_{1,\gamma} + \sum_{\eta=1}^{N_u} \hat{H}_{1,\eta} - \frac{JA}{2\nu_0} \int dz \left[\frac{1}{A} \sum_{\gamma=1}^{N_s} \hat{\xi}_{s,\gamma}(z) + \frac{1}{A} \sum_{\eta=1}^{N_u} \hat{\xi}_{u,\eta}(z) \right]^2, \quad (27)$$

where $\hat{H}_{1,\gamma}$ contains the intra-chain contributions to the energy of chain γ , such as those arising from gauche bonds and the coupling to the surface field. Self-consistent, or mean field, theory consists of approximating P_{ex} by the product of one chain probability distributions,

$$P_{ex} \approx \left(\frac{N_s}{2} \right)! \left(\frac{N_u}{2} \right)! \prod_{\gamma=1}^{N_s} \prod_{\eta=1}^{N_u} P_{s,\gamma} P_{u,\eta} \quad (28)$$

where the probability distribution of the single saturated chain is written

$$P_{s,\gamma} = \frac{1}{Q_s} \exp \left\{ -\beta \hat{H}_{1,\gamma} - \sum_k \frac{\nu_s(k)}{\nu_0} [\Pi(z_{k,\gamma}) + B_s(z_{k,\gamma}) f(\mathbf{u}_{k,\gamma} \cdot \mathbf{c})] \right\}, \quad (29)$$

$$= \frac{1}{Q_s} \exp \left\{ -\beta \hat{H}_1 - \frac{1}{\nu_0} \int [\hat{\phi}_s(z) \Pi(z) + \hat{\xi}_s(z) B_s(z)] dz \right\}. \quad (30)$$

with the fields Π and B_s to be determined, and Q_s the single saturated chain partition function

$$Q_s(\Pi, B_s) = Tr_{\{\alpha\}} \exp \left\{ -\beta \hat{H}_1 - \sum_k \frac{\nu_s(k)}{\nu_0} [\Pi(z_k) + B_s(z_k) f(\mathbf{u}_k \cdot \mathbf{c})] \right\}, \quad (31)$$

$$= Tr_{\{\alpha\}} \exp \left\{ -\beta \hat{H}_1 - \frac{1}{\nu_0} \int [\hat{\phi}_s(z) \Pi(z) + \hat{\xi}_s(z) B_s(z)] dz \right\}. \quad (32)$$

Here

$$\hat{\phi}_s(z) = \sum_{k=1}^{n_s} \nu_s(k) \delta(z - z_k), \quad (33)$$

defined previously in Eq. (2), the trace is over all configurations of a single saturated chain, and the index specifying the particular chain has been dropped. The expressions for P_u and Q_u are essentially the same except that the segment volumes are those of the unsaturated chain, and the trace is over its configurations. Note that because

$$Tr_{\{\alpha\}} P_s = 1, \quad (34)$$

and similarly for P_u , and because the sum in the normalization of the exact probability distribution, Eq. (26), is over all *distinct* states, the factor of $(N_s/2)!(N_u/2)!$ is needed in Eq. (28) so that the normalization will be satisfied within the mean field approximation.

The Helmholtz free energy of Eq. (25) can now be obtained directly within the mean field approximation of Eq. (28). One obtains

$$\begin{aligned} \frac{\beta F}{A} = & -\frac{1}{\nu_0} \int \left\{ \frac{\beta J}{2} [\rho_s \langle \hat{\xi}_s \rangle_s + \rho_u \langle \hat{\xi}_u \rangle_u]^2 + \rho_s \langle \hat{\xi}_s \rangle_s B_s(z) + \rho_u \langle \hat{\xi}_u \rangle_u B_u(z) \right. \\ & + [\rho_s \langle \hat{\phi}_s \rangle_s + \rho_u \langle \hat{\phi}_u \rangle_u] \Pi(z) \left. \right\} dz \\ & - [\rho_s \ln Q_s + \rho_u \ln Q_u] + \frac{\rho_s}{2} \ln N_s + \frac{\rho_u}{2} \ln N_u, \end{aligned} \quad (35)$$

where $\rho_s \equiv N_s/A$ and $\rho_u \equiv N_u/A$ are the areal densities of saturated and unsaturated chains,

$$\langle \hat{\phi}_s \rangle_s \equiv Tr_{\{\alpha\}} P_s \hat{\phi}_s, \quad (36)$$

and similarly for the other single-chain ensemble averages. Again chain indices have been dropped.

The unknown fields $\Pi(z)$, $B_s(z)$, and $B_u(z)$ are obtained from three conditions. The first is that the interior of the bilayer be incompressible which implies

$$\rho_s \langle \hat{\phi}_s(z) \rangle_s + \rho_u \langle \hat{\phi}_u(z) \rangle_u = 1. \quad (37)$$

The second and third are that the free energy be an extremum with respect to the undetermined functions $\langle \hat{\xi}_s \rangle_s$ and $\langle \hat{\xi}_u \rangle_u$. This leads to the equations

$$B_s(z) = B_u(z) \quad (38)$$

$$= \beta J [\rho_s \langle \hat{\xi}_s(z) \rangle_s + \rho_u \langle \hat{\xi}_u(z) \rangle_u]. \quad (39)$$

We shall denote the functions which satisfy the self-consistent Eqs. (37) to (39) as $\pi(z)$ and $b(z)$ respectively.

Substituting the fields $\pi(z)$ and $b(z)$ into the free energy, one obtains

$$\begin{aligned} \frac{\beta F}{A} = & -\rho_s \ln Q_s - \rho_u \ln Q_u + \frac{\beta J}{2\nu_0} \int dz [\rho_s \langle \hat{\xi}_s(z) \rangle_s + \rho_u \langle \hat{\xi}_u(z) \rangle_u]^2 \\ & + \frac{\rho_s}{2} \ln N_s + \frac{\rho_u}{2} \ln N_u - \frac{1}{\nu_0} \int dz \pi(z). \end{aligned} \quad (40)$$

The first two terms are simply the single chain Gibbs free energies multiplied by the number of chains per unit area. (They are Gibbs free energies as the pressure-like π is the independent variable.) These terms double-count the pairwise interaction energy, and this is corrected by the third term. The fourth and fifth terms are the entropy of mixing. Thus the first five terms are the mean field approximation for the Gibbs free energy per unit area of the system. The last term is simply $-\beta pV/A$, with p the pressure, and relates the Gibbs free energy to the Helmholtz free energy.

The contribution of the entropy of mixing can be put in a more convenient form as follows.

We note

$$(N_s \sum_k^{n_s} \nu(k) + N_u \sum_k^{n_u} \nu(k))/V = 1, \quad (41)$$

so that

$$\ln \left[\frac{N_s \sum_k^{n_s} \nu(k) + N_u \sum_k^{n_u} \nu(k)}{\nu_0} \right] = \ln \left[\frac{V}{\nu_0} \right], \quad (42)$$

where $\ln(V/\nu_0)$ is constant within the canonical ensemble. We multiply this constant by $(N_s + N_u)/2$ and subtract it from the free energy above because this term, linear in N_s and N_u , only shifts the definitions of the chemical potentials. We therefore arrive at the final expression for the mean field free energy

$$\begin{aligned} \frac{\beta F_{mft}}{A} = & -\rho_s \ln Q_s - \rho_u \ln Q_u + \frac{\beta J}{2\nu_0} \int dz [\rho_s \langle \hat{\xi}_s(z) \rangle_s + \rho_u \langle \hat{\xi}_u(z) \rangle_u]^2 \\ & + \frac{\rho_s}{2} \ln \frac{\rho_s \nu_0}{\rho_s \sum_k \nu_s(k) + \rho_u \sum_k \nu_u(k)} + \frac{\rho_u}{2} \ln \frac{\rho_u \nu_0}{\rho_s \sum_k \nu_s(k) + \rho_u \sum_k \nu_u(k)} \\ & - \frac{1}{\nu_0} \int dz \pi(z). \end{aligned} \quad (43)$$

VII. APPENDIX II. THE RIS DISTRIBUTION

This section clarifies how the sums over single lipid configurations, which are needed to evaluate single lipid ensemble averages, Eq. (15), are carried out within the rotational

isomeric states (RIS) model, and how the calculation of thermodynamic quantities is accomplished. In the RIS model⁸, the bond between the carbon at position \mathbf{r}_{k-1} and \mathbf{r}_k , $k \geq 2$, can be in one of three configurations, the lowest energy trans or the gauche plus or gauche minus with an energy higher than that of the trans by an amount ϵ_g . There can be no gauche bond between the anchoring carbon and the first carbon in the chain by definition. Further an apparent gauche bond between the first and second carbons can actually be obtained by a solid body rotation of a trans configuration. Within the RIS model, the sequence of bond orientations down the chain, the location of the anchoring carbon, \mathbf{z}_0 , and the orientation of the first normal, \mathbf{u}_1 , completely define the configuration of the chain.

The probability distribution, Eq. (29), of a saturated chain in configuration α can now be written

$$\begin{aligned} P_s(\alpha) &= \frac{1}{Q_s} \prod_{k=1}^{n_s} P_{s,k}(\alpha) \\ Q_s &= Tr_{\{\alpha\}} \prod_{k=1}^{n_s} P_{s,k}(\alpha) \\ P_{s,k}(\alpha) &= \exp(-\beta \hat{H}_{eff,k}), \end{aligned} \tag{44}$$

where the effective Hamiltonian is defined as

$$\begin{aligned} \beta \hat{H}_{eff,1} &\equiv \eta \cos(\mathbf{u}_1 \cdot \mathbf{c}) + \frac{\nu_s(1)}{\nu_0} [\pi(z_1) + b(z_1) f(\mathbf{u}_1 \cdot \mathbf{c})], \\ \beta \hat{H}_{eff,2} &= \frac{\nu_s(2)}{\nu_0} [\pi(z_2) + b(z_2) f(\mathbf{u}_2 \cdot \mathbf{c})], \\ \beta \hat{H}_{eff,k} &= g_k \epsilon_g + \frac{\nu_s(k)}{\nu_0} [\pi(z_k) + b(z_k) f(\mathbf{u}_k \cdot \mathbf{c})], \quad 2 < k \leq n_s - 1 \\ \beta \hat{H}_{eff,n_s} &= g_{n_s} \epsilon_g + \frac{\nu(n_s)}{\nu_0} \pi(z_{n_s}), \end{aligned} \tag{45}$$

where η is the surface field introduced earlier which couples to the first normal, and g_k equals unity if the bond between the carbon at \mathbf{r}_{k-1} and \mathbf{r}_k is gauche, and zero otherwise. For unsaturated lipids, the *cis*-unsaturated bond alters the bond weights. These energetic weights and configurational properties are specified in Mark¹⁸.

Not all possible bond configurations in a chain are acceptable. Those in which a gauche minus immediately follows a gauche plus or *vice versa* have large steric overlaps⁸, and are discarded. Further those configurations in which the chain intersects itself are also discarded as are those in which the chain pierces the aqueous plane and enters the region of solvent.

To carry out the sum over single lipid configurations, we first enumerate all configurations of the chains within the RIS model for a *given* position of the first monomer and orientation of the first bond. Under this constraint, the RIS configurations of these lipids are generated once and stored in a linked list with a *tree* structure. This structure allows us to store a large number of conformations and perform configurational sums using roughly a quarter of the number of operations required by a linear storage array. We then sample orientations and translations of this first bond by rotating it about the bilayer normal and then translating the chain along the bilayer normal. In particular we consider rotations of the lipid configurations as a solid body, sampling two Euler angles: that to the aqueous plane from the normal, θ , and ϕ , and about the body axis.

Translations of the whole chain normal to the bilayer are chosen in a small interval $\{-\Delta z, \Delta z\}$, with $\Delta z \sim 1.5\text{\AA}$, about the aqueous plane. We choose the first segments of the chains to originate at one of four evenly spaced locations in this window about the aqueous plane, matching a discretization of the bilayer we employ, described below. The allowed Euler rotations about the first bond varies with these origins. For example, the maximally inserted chains in this translational grid have somewhat more than the hemisphere of allowed rotations without penetrating the aqueous environment, whereas the maximally extracted ones have less than the hemisphere.

For each of these origins in the translational window, we sample the allowed solid angles. Using a shorter saturated lipid, 12 or 14 segments long, as a benchmark, we may sample both Euler angles exhaustively. A large uniform sampling, (~ 3500 total angles), indicates the dense phase has a preference for two orientations, $\theta \sim 0$, corresponding to the first bond in the *trans* state, and to a lesser extent, $\theta \sim 60^\circ$ corresponding to a first bond gauche isomerization. Since such an exhaustive sampling of angles for longer lipids is not computationally feasible, we must substantially reduce the number of angles sampled.

One way of accomplishing this is to utilize a set of angles determined from equidistant points on a sphere. This accomplishes a uniform density distribution on the sphere, each angle subtending nearly the same portion of the total solid angle. These angles are determined from a simulation of repulsive points confined to a sphere. We then increase the density of configurations for small θ , until we nearly reproduce the statistics from the exhaustive sampling above. In order to correct for the bias imposed by the selection of angles, the evaluation of the trace such as in Eq. (15) includes a factor proportional to the amount

of the total allowable solid angle they subtend. The dense set of angles near $\theta \sim 0$ each subtend a smaller amount of area and have a smaller weight.

With these rotations and translations, and discarding self-intersecting and other restricted configurations, the complete computational set includes on the order of 10^7 configurations for roughly 150 total initial bond angles for each lipid species.

To determine ensemble averages of position dependent quantities, such as

$$\hat{\phi}_{s,\gamma}(z, z_{k,\gamma}) = \sum_{k=1}^{n_s} \nu_s(k) \delta(z - z_{k,\gamma}), \quad (46)$$

of Eq. (2) or

$$\hat{\xi}_{s,\gamma}(z) = \sum_{k=1}^{n_s-1} \nu_s(k) \delta(z - z_{k,\gamma}) f(\mathbf{u}_{k,\gamma} \cdot \mathbf{c}), \quad (47)$$

of Eq. (11), we discretize the space of the continuous variable z into $2\mathcal{N}_z$ levels z_l of width $\delta z = L/2\mathcal{N}_z$. A saturated chain which is without gauche defects and which is aligned with the bilayer normal sets a limiting, maximal half-width, $L/2$, for the hydrophobic core of a one-component lipid bilayer. Typically, we divide the hydrophobic width into slices $\delta z \sim 0.75\text{\AA}$ to achieve a suitable resolution for our calculations. Free energy calculations for various bilayer widths are carried out by changing the number of slices, $2\mathcal{N}_z$, but maintaining the slice width δz . By changing the bilayer thickness incompressibly, we simply vary the average areal density of the lipids. The equilibrium states of the system are typically not among the discrete points we calculate, which may be seen in Fig. (1). Structural properties, such as the S_{CD} order parameters, are sensitive to the areal density. To estimate the order parameters, shown in Figs. (2) and (4), we first estimate the areal density of the phase from the free energy calculation, and then vary δz so that the bilayer acquires nearly the equilibrium density of the phase. In practice, changing δz slightly affects the packing of the chains in the hydrophobic core so several values of δz are used, and the order parameters are averaged over these various discretizations. This practice introduces an uncertainty in these order parameters which we estimate as ± 0.02 .

The calculation is now straightforward. For given surface compositions ρ_s and ρ_u and temperature T , the densities $\langle \hat{\phi}_s(z_l) \rangle_s$, $\langle \hat{\phi}_u(z_l) \rangle_u$, $\langle \hat{\xi}_s(z_l) \rangle_s$, and $\langle \hat{\xi}_u(z_l) \rangle_u$ are evaluated in the ensemble with the probability distribution P_s of Eq. (16) or P_u containing given fields $\pi(z_m)$ and $b(z_m)$. These fields must satisfy the self-consistent equations, Eqs. (18) and (19), which contain the densities. This set of coupled, nonlinear, equations can be

solved using a standard algorithm. Due to the mirror symmetry of the bilayer, it is sufficient to solve the self-consistent equations in the half-bilayer. To do this, chain interdigitation must be correctly accounted for in lipid configurations that extend past the midplane into the other leaf. If the configuration is long enough to interdigitate the other leaf, its monomer densities are reflected and the ‘image’ of the configuration counted in the statistics. The free energy, Eq. (14), is then calculated from which all thermodynamic information may be derived.

The parameters we have chosen for the calculations below are as follows. The saturated lipid chains we consider are $n_s = 15$ monomers long, mimicking DPPC. An interaction of strength $J/T_m = 0.09$ induces the main-chain transition at its observed value of $T_m = 315$ K. The unsaturated lipids have $n_u = 17$ monomers with a *cis-9* double bond, between the eighth and ninth segments. This is the chain structure of DOPC. For both species of lipid, we find a surface field of $\eta/k_B T_m \sim 1.03$ sufficient to obtain reasonable values of the order parameter for bonds nearest the aqueous plane.

TABLE I: Mean-Field and Experimental Results for the DPPC Bilayer. Experimental results are from Nagle and Tristram-Nagle¹⁵.

Quantity	Exp't	Mean Field
Fluid Area/lipid $T = 323$ K (\AA^2)	64.0	67.0
Gel Area/lipid $T = 293$ K (\AA^2)	47.9	49.9
Fluid Hydrophobic width $T = 323$ K (\AA)	28.5	26.7
Gel Hydrophobic width $T = 293$ K (\AA)	34.4	35.9
Gauche Bonds (gel, $T = 315$ K)		2.1
Gauche Bonds (fluid, $T = 315$ K)		4.3

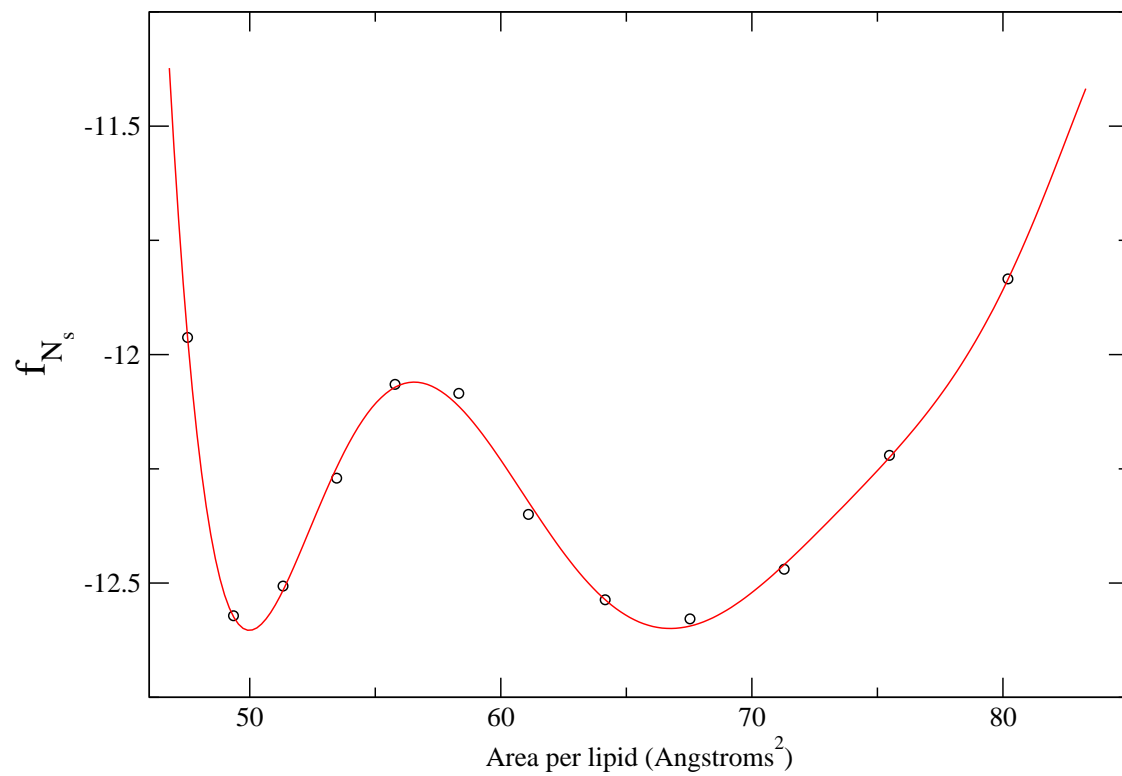
VIII. FIGURE CAPTIONS

Fig. 1 Free energy per two-chain saturated lipid, in units of $k_B T$, as a function of area per two-chain lipid. The temperature is essentially that of the main chain transition, approximately 315 K, at which the two phases are in coexistence. In each phase the surface tension, γ , vanishes. The solid line is to guide the eye.

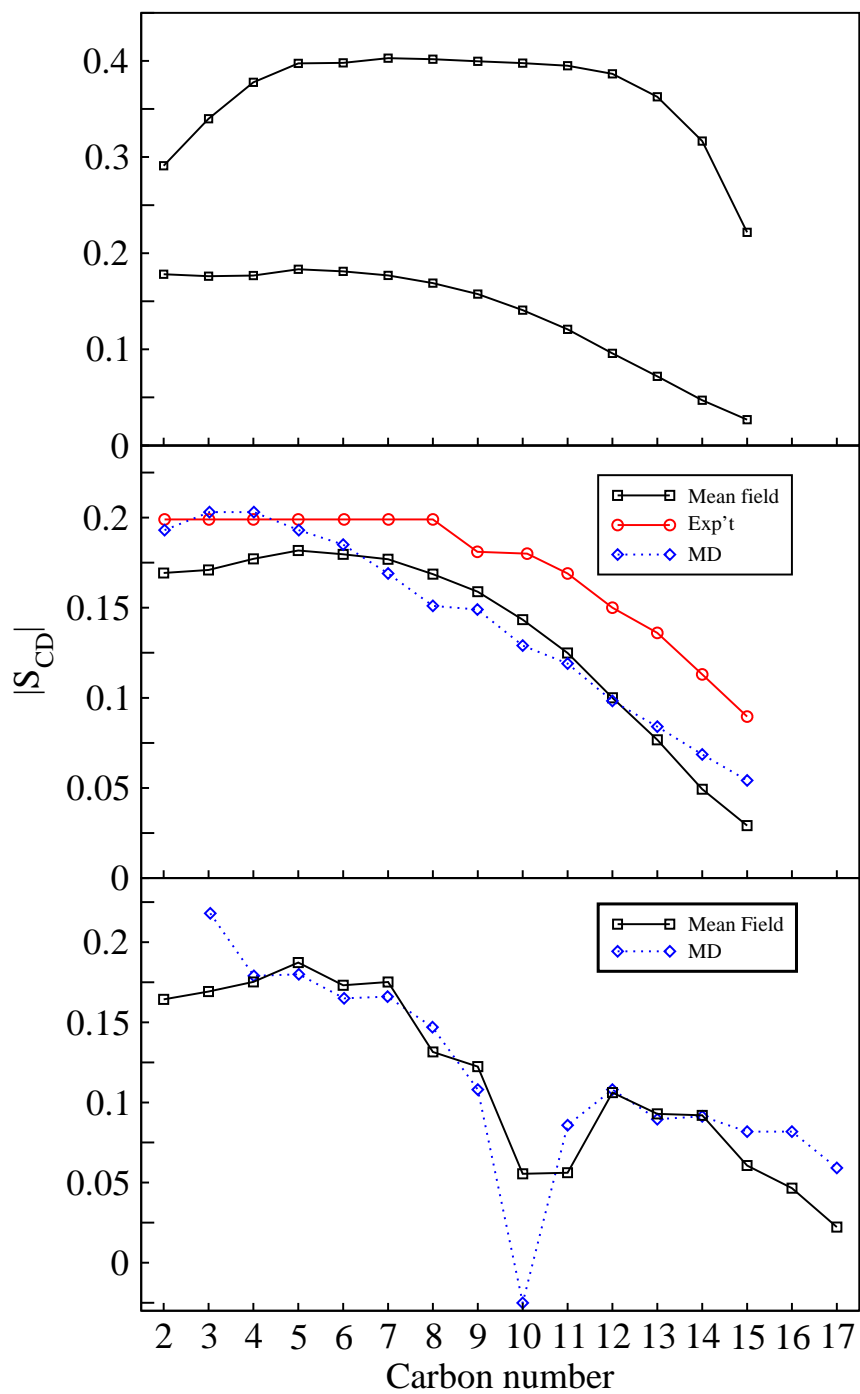
Fig. 2 Various calculated deuterium order parameters for a DPPC and a DOPC bilayer are compared with experiment and simulation. The top figure shows the calculated order parameters in coexisting liquid and gel phases for a DPPC bilayer at the transition temperature. The middle figure compares the mean-field deuterium order parameter for the fluid phase at ($T = 323$ K) to that obtained from experiment²⁴ ($T = 323$ K) and from MD simulation²⁵ ($T = 325$ K, sn-2 chains) for the fluid phase. The bottom figure compares our results for the fluid DOPC bilayer to simulation²² at $T_m = 305$ K, sn-2 chains. The indices have been shifted from the text in accord with most experiments and simulations.

Fig. 3 Calculated phase diagram for a bilayer composed of DPPC and DOPC as a function of the volume fraction of DOPC. The error bars are an estimate of the uncertainty in the calculation introduced by the bilayer discretization.

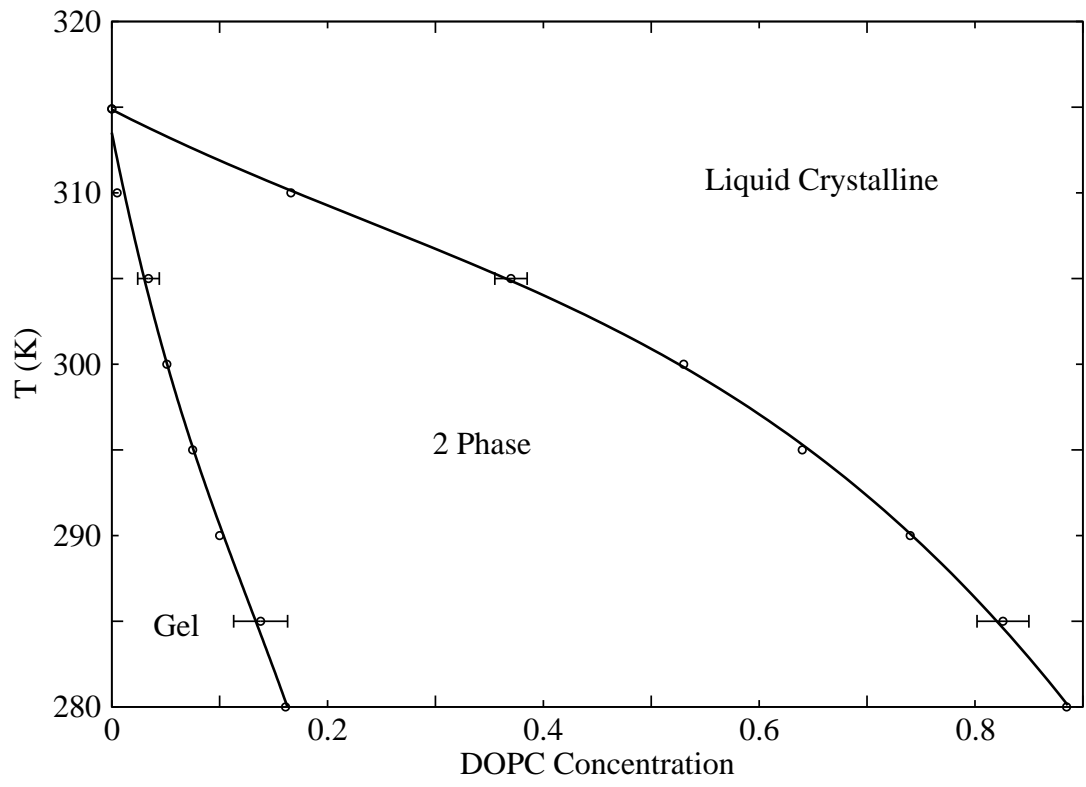
Fig. 4 Deuterium order parameters for a composite bilayer of DPPC and DOPC at $T_m = 300$ K in each of the coexisting phases. The order parameters for DOPC are identifiable by the notch half way down the chain. The upper part of the figure shows the gel phase order parameters, and the lower part shows the liquid phase order parameters. The indices have been shifted from the text in accord with most MD simulations



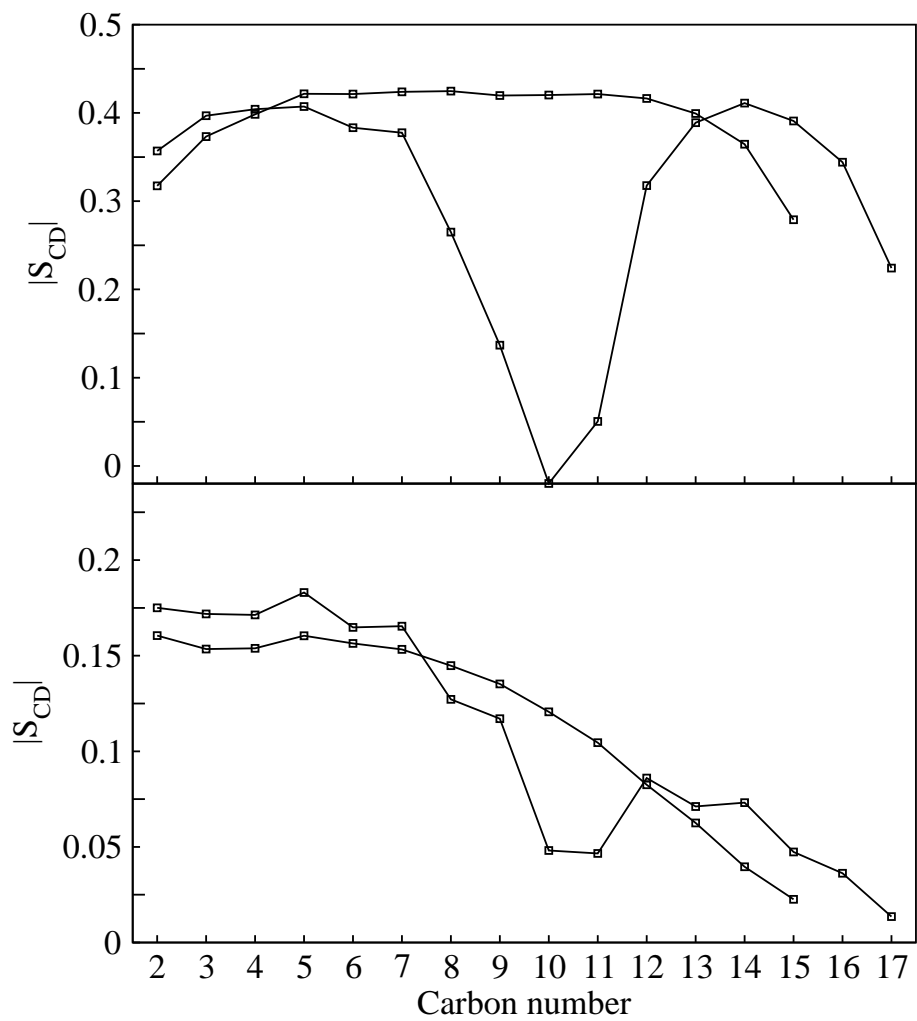
R. Elliott et. al, Fig. 1



R. Elliott et. al, Fig. 2



R. Elliott et. al, Fig. 3



R. Elliott et. al, Fig. 4

¹ M. Edidin, Annu. Rev. Biophys. Biomol. Struct. **32**, 257 (2003).

² S. L. Veatch and S. L. Keller, Phys. Rev. Lett. **89**, 268101 (2002).

- ³ S. L. Veatch and S. L. Keller, *Biophys. J.* **85**, 3074 (2003).
- ⁴ C. Dietrich, L. A. Bagatolli, Z. N. Volovyk, N. L. Thompson, M. Levi, K. Jacobson, and E. Gratton, *Biophys. J.* **80**, 1417 (2001).
- ⁵ T. Y. Wang and J. R. Silvius, *Biophys. J.* **81**, 2762 (2001).
- ⁶ J. H. Ipsen, G. Karlstrom, O. G. Mouritsen, H. Wennerstrom, and M. J. Zuckermann, *Biochim. Biophys. Acta.* **905**, 162 (1987).
- ⁷ M. Nielsen, L. Miao, J. H. Ipsen, M. J. Zuckermann, and O. G. Mouritsen, *Phys. Rev. E.* **59**, 5790 (1999).
- ⁸ P. J. Flory, *Statistical Mechanics of Chain Molecules* (Wiley-Interscience, New York, 1969).
- ⁹ A. Ben-Shaul, I. Szleifer, and W. Gelbart, *J. Chem. Phys.* **83**, 3597 (1985).
- ¹⁰ D. W. R. Gruen, *Biochim. Biophys. Acta* **595**, 161 (1979).
- ¹¹ I. Szleifer, A. Ben-Shaul, and W. M. Gelbart, *J. Chem. Phys.* **85**, 5345 (1986).
- ¹² D. R. Fattal and A. Ben-Shaul, *Biophys. J.* **67**, 983 (1994).
- ¹³ C. Tanford, *The Hydrophobic Effect, 2nd ed.* (Wiley, New York, 1980).
- ¹⁴ R. S. Armen, O. D. Uitto, and S. E. Feller, *Biophys. J.* **75**, 734 (1998).
- ¹⁵ J. F. Nagle and S. Tristram-Nagle, *Biochim. Biophys. Acta* **1469**, 159 (2000).
- ¹⁶ F. Schmid, *J. Phys.: Condens. Matter* **10**, 8105 (1998).
- ¹⁷ S. Marcelja, *Biochim. Biophys. Acta* **367**, 165 (1974).
- ¹⁸ J. E. Mark, *Physical Properties of Polymers Handbook* (AIP Press, Woodbury, New York, 1996).
- ¹⁹ L. Finegold and M. Singer, *Biochim. Biophys. Acta.* **855**, 417 (1986).
- ²⁰ S. Feller, D. Yin, R. W. Pastor, and J. A. MacKerell, *Biophys. J.* **73**, 2269 (1997).
- ²¹ R. J. Mashl, H. L. Scott, S. Subramaniam, and E. Jakobsson, *Biophys. J.* **81**, 3005 (2001).
- ²² S. W. Chiu, E. Jakobsson, S. Subramaniam, and H. L. Scott, *Biophys. J.* **77**, 2462 (1999).
- ²³ B. R. Lentz, Y. Barenholz, and T. E. Thompson, *Biochemistry* **15**, 4529 (1976).
- ²⁴ H. I. Petrache, S. W. Dodd, and M. F. Brown, *Biophys. J.* **79**, 3172 (2000).
- ²⁵ S. W. Chiu, M. M. Clark, E. Jakobsson, S. Subramaniam, and H. L. Scott, *J. Comp. Chem.* **20**, 1153 (1999).